Supplementary Information

Glacial buzzcutting limits the height of tropical mountains

This document 1) gives raw analytical data used in exposure age calculation and presents alternative age estimates for different scaling schemes and production rates and, 2) shows field evidence of glacial features and escarpments at Cerro Chirripó and Nanhudashan, 3) presents a geological map of Cerro Chirripó and 4) adds expanded hypsometric analysis.

S1. ^{10}Be Raw data

^{10}Be exposure age dating analysis

DR Table 1. Geographical and analytical data for the samples from Chirripó

Sample ID	CAMS laboratory no.	Lat.	Long.	Elev. (m)	Thickness (cm)	Topographic Shielding	Mass (g)	Be Carrier (g)	^{10}Be/^{9}Be (10^{-14})	^{10}Be Conc. (10^{4} atm/g)	^{10}Be/^{9}Be ratio standard
VMR-14-01	BE38094	9.50002	-83.48929	3481	2.47	0.986	5.0076	0.1874944	14.7873 ± 0.2374	37.1591 ± 0.5868	07KNSTD
VMR-14-02	BE38095	9.49426	-83.48659	3497	0.75	0.987	5.0061	0.1882112	15.2234 ± 0.2818	38.3532 ± 0.6985	07KNSTD
VMR-14-03	BE38096	9.4998	-83.48961	3470	0.85	0.985	5.0503	0.1873920	15.7785 ± 0.2923	39.2368 ± 0.7152	07KNSTD
VMR-14-04	BE38097	9.50518	-83.49237	3417	0.69	0.967	5.0570	0.1880064	14.9551 ± 0.3521	37.4769 ± 0.8500	07KNSTD
VMR-14-05	BE38098	9.5062	-83.49303	3393	0.42	0.968	5.0440	0.1873920	15.4086 ± 0.2471	38.4477 ± 0.6065	07KNSTD
VTL-14-02	BE38103	9.45346	-83.50319	3425	1.25	0.989	5.0159	0.1856512	1.49129 ± 0.2397	37.1071 ± 0.5862	07KNSTD
MCH-14-03	BE38100	9.48582	-83.49130	3759	1.01	0.987	5.0321	0.1871872	22.4575 ± 0.4156	55.9493 ± 1.0186	07KNSTD
MCH-14-02	BE38102	9.48461	-83.48900	3814	0.88	0.997	1.5524	0.1871872	2.88263 ± 0.0951	23.3869 ± 0.7673	07KNSTD
MCH-14-01	BE38099	9.4832	-83.48698	3674	6.08	0.872	3.4982	0.1873920	8.81571 ± 0.1635	31.6230 ± 0.5771	07KNSTD
BLK1-2014Oct23								0.1869824	0.01653 ± 0.0080		

Table S1. A procedural blank was processed identically with these samples, and is listed at the end of the table. Results are given with 1σ analytical AMS uncertainties. We used a Garmin eTrex handheld GPS to record altitude and position (WGS84). Samples were measured with a Be carrier concentration of 1024 ppm. AMS ratio and Be concentration data presented in this table as originally measured against the specified standard in the last column. Reported values are corrected for background ^{10}Be detected in associated procedural blank listed below samples. Reported ^{10}Be/^{9} Be value for 07KNSTD standard material is ^{10}Be/^{9}Be=2.85×10^{-12}, respectively (Nishiizumi et al., 2007; ^{10}Be half life = 1.36 Myr).

	Kelly et al., 2014		**Blard et al., 2013**	
Sample ID	St age	Lm age	St age	Lm age
VMR-14-01	16900 ± 500	16300 ± 500	16000 ± 900	15800 ± 1000
VMR-14-02	17100 ± 500	16500 ± 500	16200 ± 300	15900 ± 1000
VMR-14-03	17700 ± 500	17100 ± 500	16800 ± 900	16500 ± 1000
VMR-14-04	17600 ± 600	17000 ± 600	16700 ±1000	16400 ± 1100
VMR-14-05	18300 ± 500	17600 ± 500	17400 ± 1000	17000 ± 1100
MCH-14-01	15200 ± 500	14800 ± 400	14400 ± 800	14300 ± 900
MCH-14-03	22000 ± 700	20800 ± 600	20900 ± 1200	20000 ± 1300
MCH-14-02	8750 ± 400	8400 ± 300	8300 ± 500	8000 ± 600
VTL-14-02	17100 ± 500	16500 ± 500	16200 ± 900	16000 ± 1000

Table S2. Production rates determined by Kelly et al. (2013) and Blard et al. (2013). Age uncertainties include internal analytical error and propagation of the procedural blank error in quadrature. The discussion in the main text is based on St ages and the Kelly et al. (2013) production rate, although our conclusions are unaffected by choice of scaling model given that these ages indicate substantial glacial retreat near the end of the gLGM.

S2. Field data from Chirripó and Nanhudashan

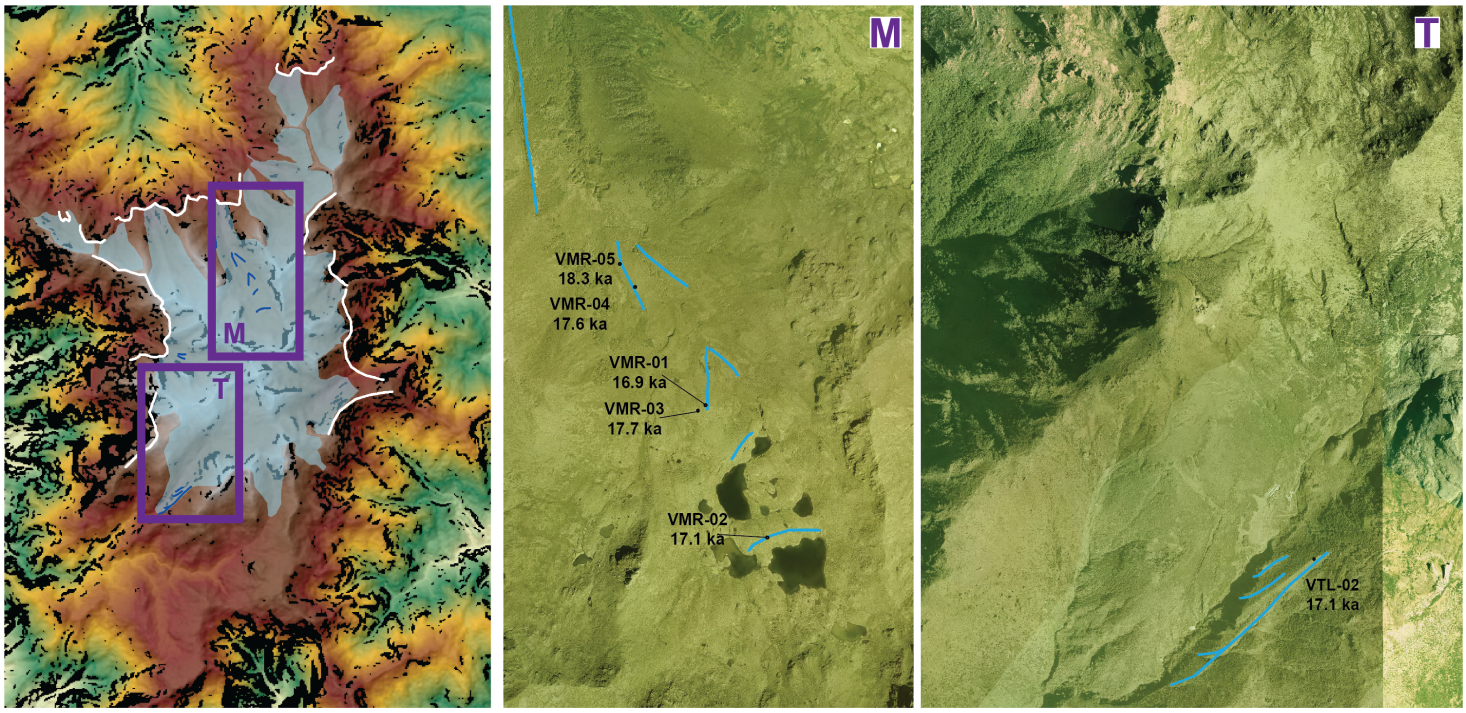

Figure S1. Moraine boulder ages with geomorphic context. Left is original map from main text Fig. 1. Box M indicates Valle de las Morrenas, box T indicates Valle Talari. Moraines in dark blue on context map, and in light blue on images M and T. In Valle de las Morrenas moraine boulders gave ages that decreased toward the headwall. Aerial images courtesy of Costa Rica Sistema Nacional de Áreas de Conservacion (SINAC).

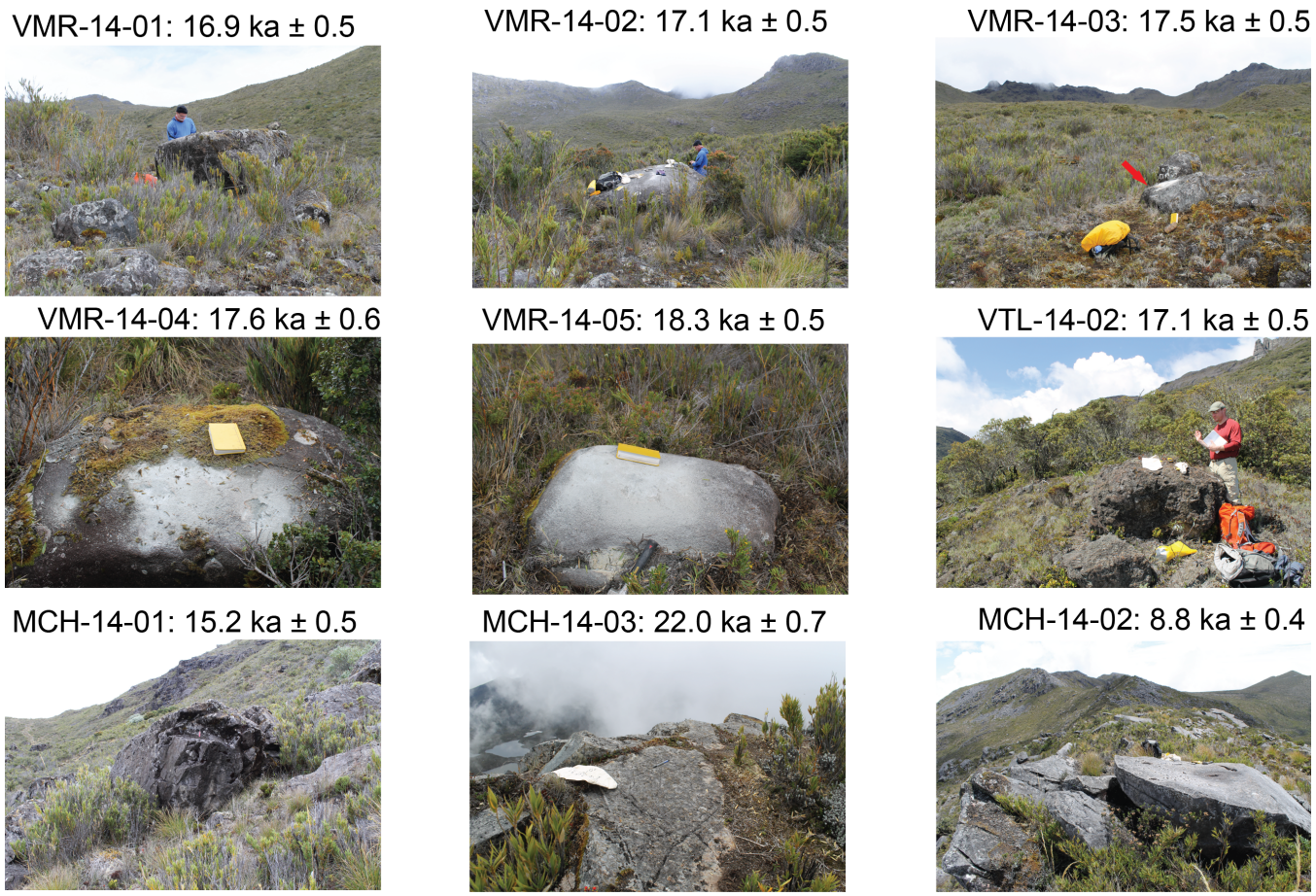

Figure S2. ^{10}Be exposure age surfaces. VMR-14-01 through VMR-14-05 are diorite moraine boulders in Valle de las Morrenas. VTL-14-02 is a quartz-bearing andesitic moraine boulder in Valle Talari. All are highlighted in light blue in main text Fig. 1. VMR-14-04/05 and VTL-14-02 come from lateral moraines, VMR-14-01/02/03 come from hummocky moraines in the Valle de las Morrenas cirque. MCH-14-02 is a landslide/rock avalanche boulder along the headwall of Valle Pirámide, and is highlighted in purple in main text Fig. 1. MCH-14-01 is a scoured surface near the Chirripó summit, but we suspect that it sustained intermittent cover post ice-retreat, and therefore yielded an unrealistic deglaciation age. MCH-14-02 is a bedrock surface along the ridge between Valle de los Lagos and Valle de las Morrenas. The two bedrock surfaces are highlighted in red in main text Fig. 1.

Field photos for scarps, glacial features

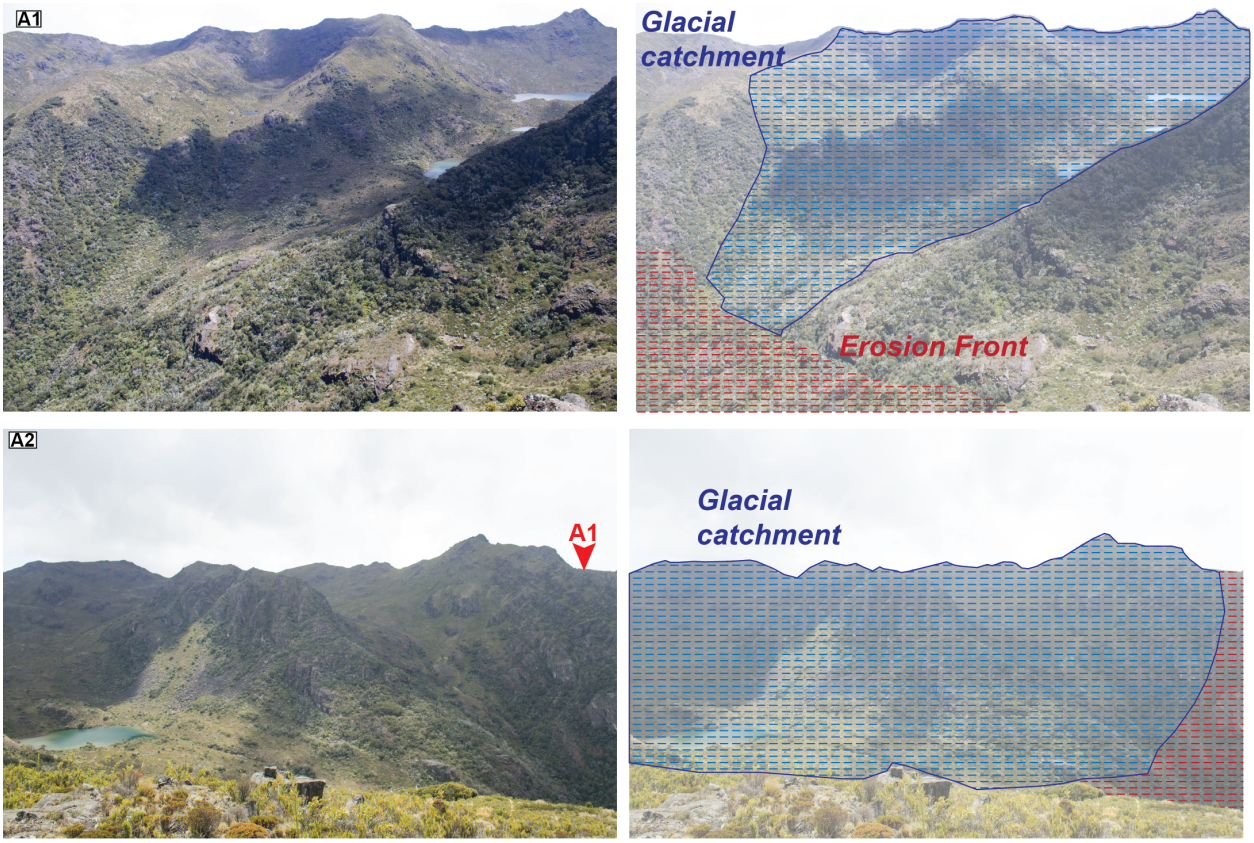

Figure S3A1-2: Valle de los Lagos erosion fronts. A1, looking N, A2 looking S. Dashed red lines indicate the position of erosion fronts, which correspond to white lines on in Fig. 1.

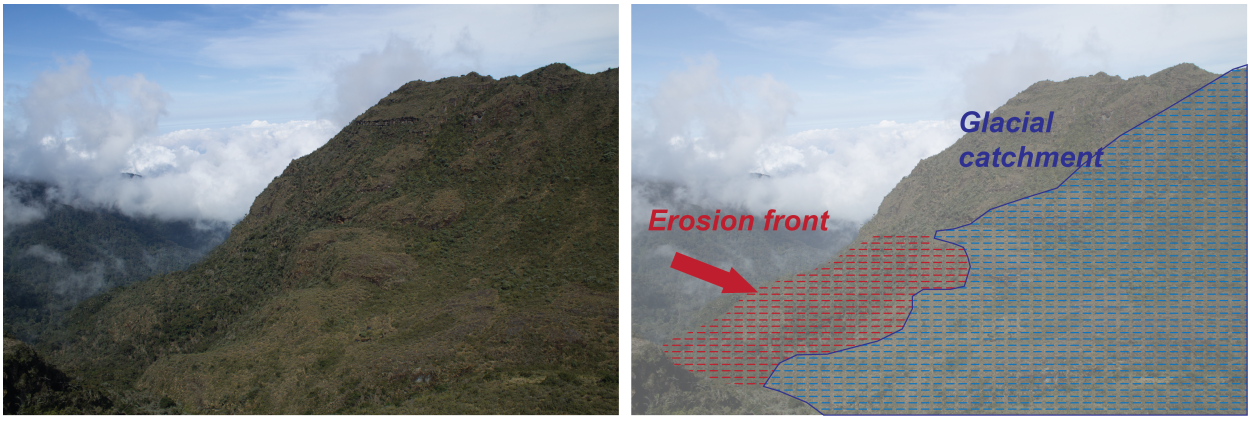

Figure S4: Valle Truncado erosion front. Fieldwork confirms that the area is blue was glacially scoured, and contains glacial erratics.

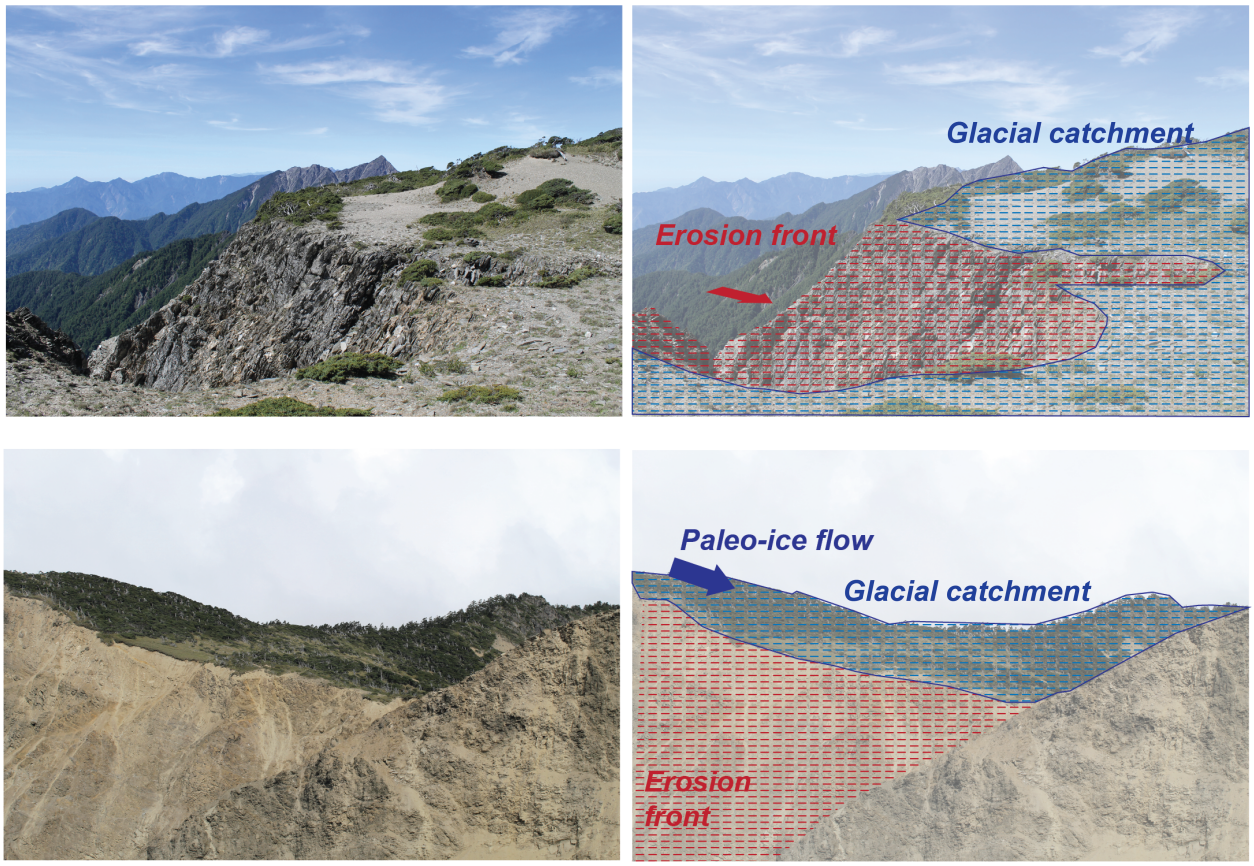

Figure S5: Erosion fronts at Nanhu SE (**top**) and Nanhu NE.

Figure S6. Striated bedrock at ~3500 m in Valle Talari, at the base of a low-sloping cirque floor. Yellow tape measure is 0.5 m.

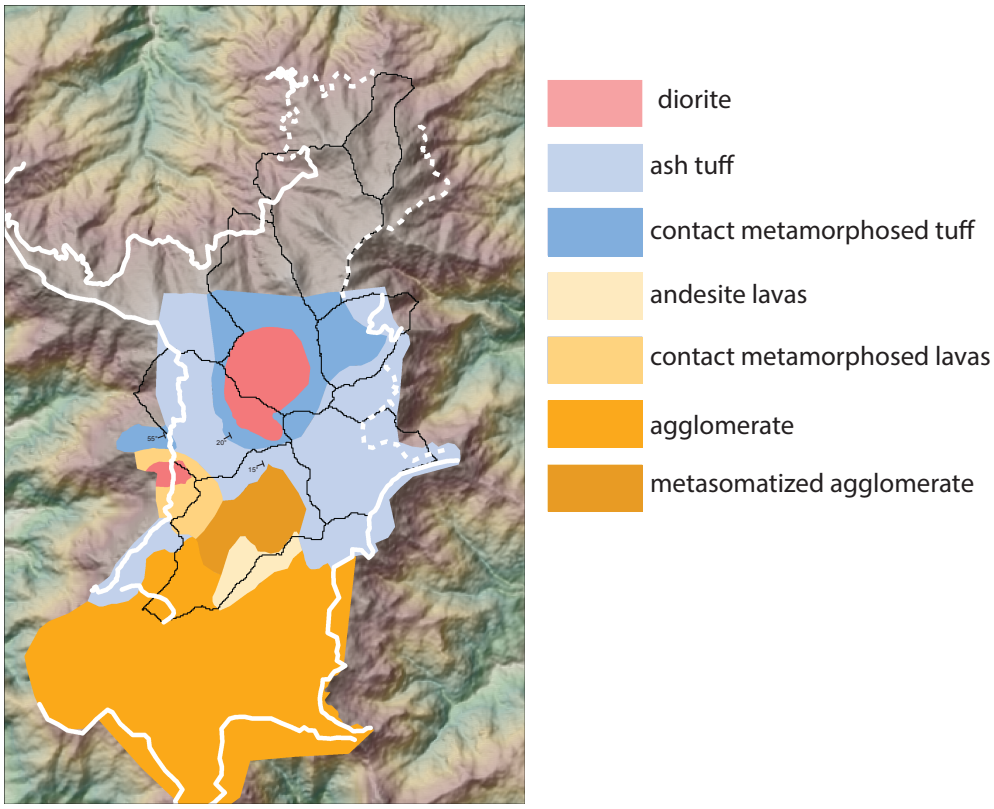

Figure S7. The Chirripó massif is composed of pyroclastics and intermediate lavas and intrusives. A diorite pluton emplaced during the late Miocene (Morell et al., 2012) has contact metamorphosed volcanic rocks. Catchment outlines are the same as those in Fig. 2 in the main text. Lithology cannot reasonably explain the observed variation in ERME. For example, the diorite that has contact metamorphosed pryoclastics and lavas is exposed along the ridge between Valle de las Morrenas Valle Lagos and along the floor of both valleys, which have an ERME of 0.8 m and 139 m, respectively.

Extended hypsometric analysis

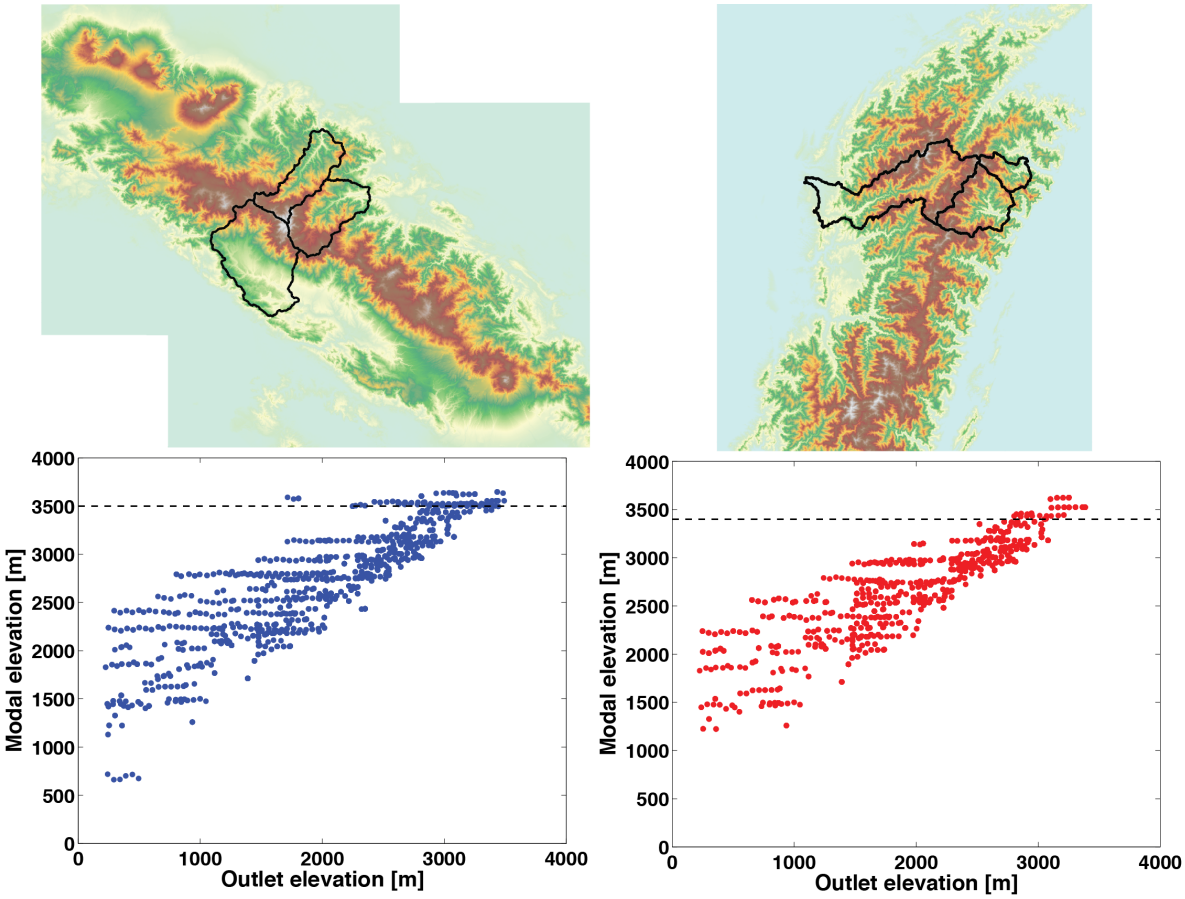

Figure S8. *Top*: Large catchments (outlet at 250 m) capped by glaciated valleys in Costa Rica (left) and Taiwan (right). Hypsometric maxima of these large areas are below the LGM ELA (DR Fig. 10). *Bottom*: catchment hypsometries for different outlet elevations. Vertical axis is the hypsometric maximum (modal average elevation) for every catchment draining to an outlet on the horizontal axis. This analysis reveals hypsometric maxima that persist for catchments of increasing outlet elevation (horizontal strings of points), but the highest of these geomorphic features are glacial benches near the LGM ELA. Importantly, even catchments with low outlets (e.g. 1500 m) have hypsometric maxima near the ELA.

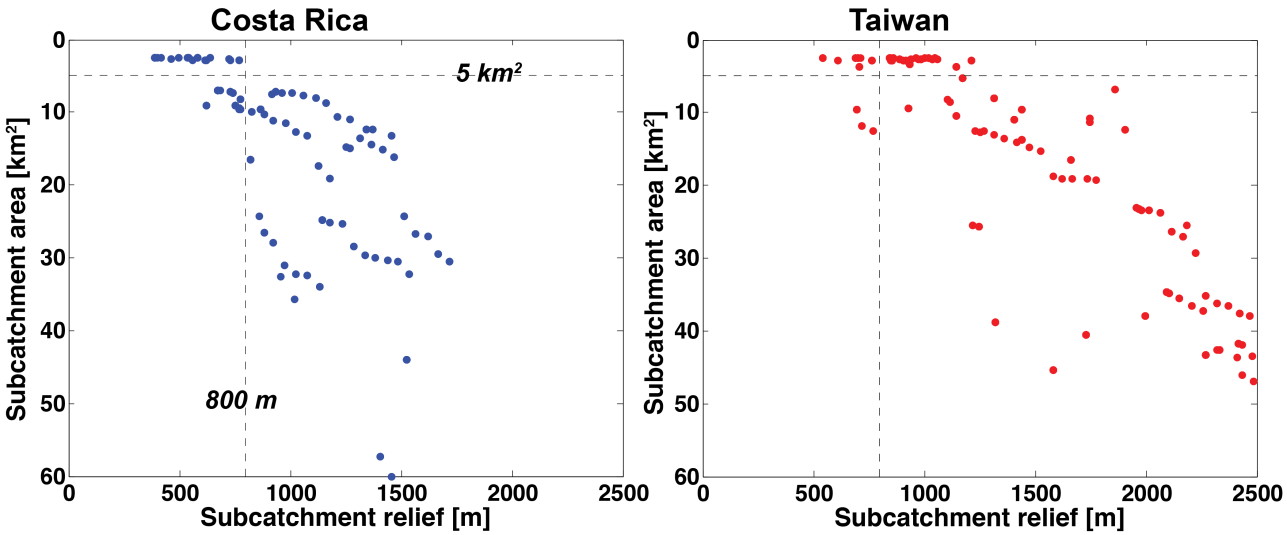

Figure S9. Catchment relief vs. catchment area. We sought a catchment relief that would isolate glaciated catchments and cover a range of elevations above and below the estimated LGM ELA of 3500 m in Costa Rica. We found that a catchment relief of 800 m was a good compromise between focused hypsometric analysis and a substantial elevation range for Costa Rica (left). We isolated catchments with the same relief in Taiwan.

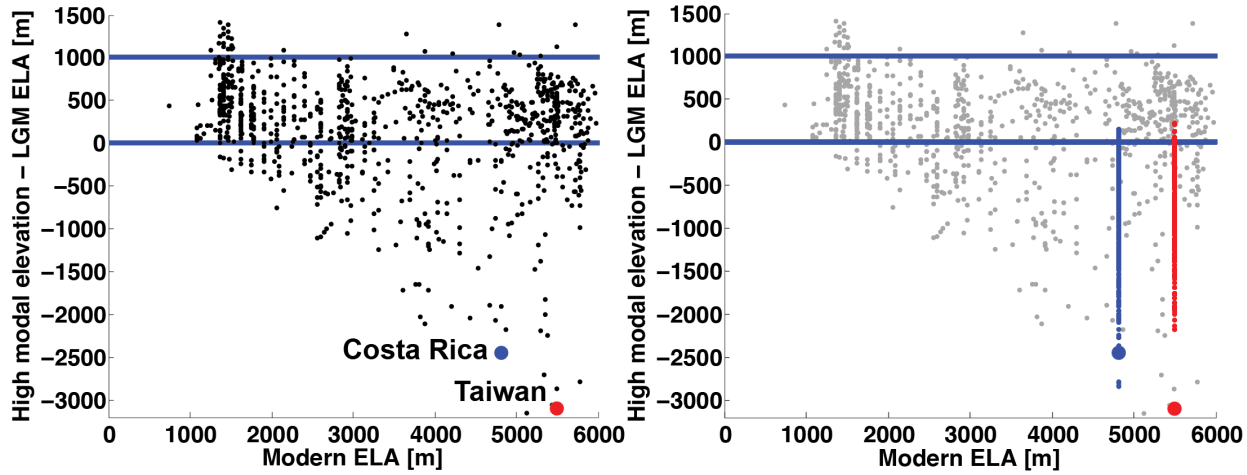

Figure S10. Adapted from Egholm, et al., 2009, Fig. 2. *Left*: global distribution of hypsometric maxima from 1° lat x 1° SRTM tiles referenced to the LGM ELA (0 on y-axis indicates is hypsometric maxima at the LGM ELA). Costa Rica in blue, Taiwan in red. Right: catchment hypsometric maxima from DR. Fig 7 are collapsed onto the x-axis, showing that some catchments in these places have hypsometric maxima near the LGM ELA.